# Effect of Nitration on the Physicochemical and Kinetic Features of Wild-Type and Monotyrosine Mutants of Human Respiratory Cytochrome *c*[†]

Vicente Rodríguez-Roldán, José Manuel García-Heredia, José A. Navarro, Miguel A. De la Rosa, and Manuel Hervás*

*Instituto de Bioquímica Vegetal y Fotosíntesis, Centro de Investigaciones Científicas Isla de la Cartuja, Universidad de Sevilla and Consejo Superior de Investigaciones Científicas, Sevilla, Spain*

*Received July 15, 2008; Revised Manuscript Received October 2, 2008*

ABSTRACT: The effect of tyrosine nitration on the physicochemical properties and reactivity of human respiratory cytochrome *c* has been extensively analyzed. A set of mutants, each bearing only one tyrosine out of the five present in the wild-type molecule, has been constructed in order to study the effect of each tyrosine nitration on the properties of the whole protein. Replacement of tyrosines by phenylalanines does not promote significant changes in the properties of the cytochrome. Nitration of wild-type cytochrome *c* promotes a drastic decrease (ca. 350 mV) in the midpoint redox potential, probably induced by nitration of both tyrosines 48 and 67. Nitration also promotes a significant decrease in the intrinsic reactivity of all the wild-type and mutant proteins. Nitration of mutant cytochromes and, in particular, of the wild-type protein significantly decreases their reactivity with cytochrome *c* oxidase, thereby suggesting that this alteration is due to an accumulative effect of different nitrations. The reactivity of mutants bearing tyrosine 67 and, to a lesser extent, tyrosine 74 is more affected by nitration, indicating that the change in reactivity of nitrated wild-type cytochrome *c* is mainly due to nitration of these tyrosine residues. Moreover, nitration of wild-type cytochrome *c* induces a significant loss in its ability to activate caspases because of the additive effect of nitration of several tyrosine groups, as inferred from the behavior of monotyrosine mutants.

Respiratory cytochrome *c* (C*c*)[1] is a small (ca. 12 kDa), soluble protein located in the mitochondrial intermembrane space, where it serves as a mobile carrier in the respiratory chain, shuttling electrons between the membrane-embedded complexes cytochrome $bc_1$ and cytochrome *c* oxidase (C*c*O). Mitochondria are one of the main sources of reactive nitrogen and oxygen species (RNOS) in the cell, and these two membrane complexes are actively involved in the production of such species (*1, 2*).

In addition to the well-established role of the mitochondria in energy metabolism, regulation of cell death has emerged as a second major function of these organelles (*3*). This, in turn, seems to be intimately linked to their role as the major intracellular source of RNOS. Excessive RNOS production can lead to oxidation of macromolecules and, subsequently, to mitochondrial DNA mutations, aging, and cell death. Mitochondria-generated RNOS seem to play an important role in the release to the cytoplasm of C*c* and other pro-apoptotic proteins, which can trigger caspase activation and apoptosis (*3*). After leaving the mitochondria, C*c* binds to Apaf-1 and forms the apoptosome complex, thus acting as an activator of the caspase-dependent apoptotic route, which in turn drives cells to death (*4*−*6*).

Among other possibilities, protein nitration is one of the most common effects of RNOS in the cell. Although this process is not enzymatically catalyzed, it is indeed very specific, as only a few residues (mainly tyrosines) are preferentially nitrated (*7*−*10*). C*c* is a main target for RNOS in mitochondria, where it is both nitrated and nitrosylated in vivo (*11*−*14*). There is contradictory information on the role of nitrated C*c* in apoptosis. Thus, it has been suggested that nitrated C*c* could act as an apoptotic signaler and that the modified protein has an enhanced ability for exit from the mitochondria (*2, 15, 16*). Other studies, however, indicate that the apoptosome assembly is initiated by the native, unmodified C*c* and that the nitrated protein possesses a reduced ability to activate caspases (*17, 18*). Moreover, the existence of a denitration system in vivo has been proposed (*19, 20*), opening the possibility that nitration could be used by the cell as a signaling system similar to phosphorylation or alkylation.

Although the sequence homology among respiratory C*c*s is very high, human C*c* shows a unique behavior in its reactivity with horse C*c*O as compared with horse and plant

[†] This work was supported by grants from the Spanish Ministry of Science and Innovation (BFU2006-01361) and the Andalusian Government (PAIDI, BIO-0198).

* Corresponding author: tel 34-954-489-514; fax 34-954-460-065; e-mail mhervas@us.es.

[1] Abbreviations: AFU, arbitrary fluorescence units; C*c*O, cytochrome *c* oxidase; C*c*, cytochrome *c*; CHAPS, 3-[(3-cholamidopropyl)-dimethylammonio]-1-propanesulfonic acid; dRf, 5-deazariboflavin; DTT, dithiothreitol; EDTA, ethylenediaminetetraacetic acid; EGTA, ethylene glycol bis(β-aminoethyl ether)-*N*,*N*,*N*′,*N*′-tetraacetic acid; FMN, flavin mononucleotide; HEPES, *N*-(2-hydroxyethyl)piperazine-*N*′-ethanesulfonic acid; $k_2$, second-order rate constant; $K_A$, equilibrium constant for complex formation; $k'_{et}$, apparent electron-transfer rate constant; $k_{obs}$, observed pseudo-first-order rate constant; LF, lumiflavin; MALDI-TOF, matrix-assisted laser desorption ionization time of flight; PCR, polymerase chain reaction; RF, riboflavin; RNOS, reactive nitrogen and oxygen species; WT, wild type.

10.1021/bi801329s CCC: $40.75 
Published on Web 11/01/2008

Ccs. In fact, human C*c* shows an apparent electron transfer rate constant ($k'_{et}$) that is ca. 5−7 times lower than those of the two other Ccs at low ionic strength (*21*). The apparent contradiction of human C*c* being less reactive than the plant protein with animal C*c*O can be explained in the light of specific evolutionary changes of both C*c*O and C*c* in primates (*22*).

Although there are previous studies on the effect of nitration on the properties of C*c*, most of these studies have been done with a mixture of nitrated and native protein, and thus reliable results on the specific effect of nitrating different positions could not be attained (*8*). However, by use of purified C*c* nitrated at different positions, it has been recently shown that nitration of tyrosine 97 has little effect on the properties of C*c* as compared to nitration at other positions (*23, 24*).

Among the changes induced by nitration, the following have been reported: (i) spectral changes indicating the loss of iron coordination of Met80, (ii) an increase in peroxidase activity associated with the change of coordination, and (iii) a noticeable decrease in the capability of nitrated C*c* to sustain respiratory electron flow in isolated mitochondria (*8, 23*). A decrease in the redox potential after nitration has also been reported, although a particular value for the potential was not determined because of reduction of the nitro group to the amino species by the chemical reductants used (*16, 18*). Recently, the increased peroxidase activity of nitrated C*c* has been related to nitration and oxidation of other biomolecules (*16*); moreover, a certain decrease in the ability of nitrated C*c* to reduce isolated C*c*O has been observed by measuring oxygen consumption under steady-state conditions (*16*).

In this work, the effect of nitration of human C*c* has been extensively examined by analyzing several physicochemical properties of the nitrated protein as well as its reactivity toward flavins and isolated horse C*c*O via time-resolved spectroscopy. Moreover, the ability of nitrated C*c* to activate caspases has also been studied. In order to determine the effect of nitration of each individual tyrosine, five mutants of C*c* have been also constructed, each one bearing only one out of the five tyrosines of the native protein.

## EXPERIMENTAL PROCEDURES

*DNA Techniques.* Plasmid pCytH, containing the region coding for human respiratory C*c* (h-C*c*) fused to the signal peptide of *Nostoc* sp. PCC 7119 cytochrome $c_6$, was constructed as described in ref *21*. From this plasmid, the different monotyrosine mutants of C*c* have been obtained by performing six mutagenic PCR steps with the Stratagene QuickChange mutagenesis kit according to manufacturer instructions. To obtain the different mutants, oligonucleotides of 21 base pairs with the following codon changes were used: TAT to TTT for mutations Y48F, Y74F, and Y97F; TAC to TTC for mutations Y46F and Y67F; TTC to TAC for the reverse mutations F46Y and F67Y; and TTT to TAT for the reverse mutation F74Y. In the first five steps, each tyrosine of the gene was mutated, one by one, to phenylalanine, in order to obtain a mutant without any tyrosine, the so-called "null mutant" (h-Null). In the last step, and starting from the null mutant, the different phenylalanines were mutated, one by one, to tyrosines to generate the five mutants each bearing a single tyrosine. Incorporation of the desired mutations and absence of any additional change were checked by sequencing the mutated constructs.

*Obtaining Cell Extracts.* Jurkat cells were maintained in RPMI (PAA) medium supplemented with 9% fetal bovine serum (BioWhitaker), 100 $\mu$g mL$^{-1}$ penicillin, 100 $\mu$g mL$^{-1}$ streptomycin, and 2 mM L-glutamine (Gibco). Cell extracts were obtained from cultures grown up to a density of 2 × 10$^6$ cells mL$^{-1}$, as described in ref *25*.

To remove endogenous C*c*, the cell extracts were treated with carboxymethylcellulose (CM-cellulose) for 10 min at 4 °C with gentle stirring. After treatment, the suspension was centrifuged twice at 12000*g* for 10 min, and the supernatant was treated again with CM-cellulose as before. The absence of C*c* in the extracts was confirmed by Western blot. Finally, the extracts were distributed into aliquots, frozen with liquid $N_2$, and stored at −80 °C.

*Synthesis of Peroxynitrite and Nitration of Proteins.* The synthesis of peroxynitrite and nitration of the different C*c* species was performed as previously described (*8*), with minor modifications. The nitration solution contained 200 $\mu$M C*c* in 1 mM $Fe^{3+}$-EDTA, 1 mM ferricyanide, and 250 mM potassium phosphate, pH 7.0. To this solution, seven bolus additions of peroxynitrite were done to a final concentration of 3 mM, with 3 min time spacing between them. The presence of $Fe^{3+}$-EDTA in the nitration solution enhances the rate and extent of tyrosine nitration because the metal ions appear to catalyze the heterolytic cleavage of peroxynitrite to form a nitronium-like species ($NO_2^+$), which is an efficient nitrating agent (*26*). In all cases the final ratio peroxynitrite/$H_2O_2$ in the peroxynitrite preparations was higher than 300, so less than 10 $\mu$M $H_2O_2$ was added to the samples in the nitration procedure. After nitration, the cytochrome was washed twice with 10 mM potassium phosphate, pH 7.0, and purified as described below.

*Production of Recombinant Proteins and Purification Procedures.* Production and purification of the different C*c* variants was performed as previously described for the wild-type (WT) protein (*21*). Protein concentration was determined spectrophotometrically with absorption coefficients of 31.7 mM$^{-1}$ cm$^{-1}$ at 549.5 nm for reduced h-WT C*c* (*21*) and h-Y67 mutant and 32.0 mM$^{-1}$ cm$^{-1}$ at 551 nm for the rest of mutants. Purity of the resulting protein fractions was determined by use of an $A_{279}/A_{551}$ ratio of ca. 0.95 for pure h-WT C*c* and verified by MALDI-TOF analysis. Nitrated C*c* was separated from nonnitrated protein on a CM-cellulose column equilibrated with 1.5 mM borate, pH 9.0, with a 0−100 mM NaCl continuous gradient. Nitrated fractions eluted with much lower concentrations of salt than native proteins, due to the extra negative charge of the deprotonated tyrosyl anions, the p$K_a$ of which is altered by the strongly electron-withdrawing effect of the $NO_2$ substituent group when in the 3-position (*2, 8*). The purity of nitrated C*c* preparations was confirmed by MALDI-TOF analysis, with only a band of the expected weight for nitrated C*c* being found.

Horse heart C*c*O was purified as described by Soulimane and Buse (*27*) with the following modifications: after a first Q-Sepharose chromatography, two additional ammonium sulfate fractionation steps (25% and 50%) were included. C*c*O concentration was determined by use of a differential extinction coefficient $\Delta\varepsilon_{604-630}$ of 17 mM$^{-1}$ cm$^{-1}$ for the reduced minus oxidized protein, as reported for the bovine

enzyme (*28*). Horse heart C*c* (e-C*c*) was purchased from Sigma and used without further purification.

*Analytical Methods.* Molecular masses were determined by MALDI-TOF (Brüker-Daltonics, Germany) analysis via standard procedures. Redox titrations were performed in a Hewlett-Packard 8452A diode-array spectrometer with a Pt−Ag/AgCl combined electrode (Microelectrodes, Inc.) as described previously (*21*). For determination of the redox potential of nitrated C*c*, and to avoid the reduction of the nitro groups by dithionite (*29*), phototitration in the presence of 2 $\mu$M 5-deazariboflavin (dRf) and 2 mM EDTA was performed (*30*). Short pulses of white light generated, in the presence of EDTA, flavin semiquinone, which in turn reduces the C*c* without altering the nitro group. Differential absorbance change was monitored at 550 minus 528 nm for native C*c* and at 550 minus 524 nm for nitrated C*c*. For low-potential determinations, 10 $\mu$M anthraquinone-2-sulfonate, 10 $\mu$M duroquinone, and 5 $\mu$M phenazine methosulfate were used as redox mediators. Extinction coefficients were determined as described previously (*31*). Circular dichroism (CD) spectra were recorded with a MOS-450 AF/CD multipurpose spectrophotometer (Bio-Logic, France) in a 1 mm quartz cuvette at 25 °C. Protein concentration was 40 $\mu$g mL$^{-1}$ in 10 mM sodium phosphate buffer, pH 7.0. Spectra were analyzed with the CDpro software package (*32*) with reference set 7 (48 proteins).

*Kinetic Analysis.* For analysis of C*c* reduction by flavin semiquinones, the laser-flash photolysis apparatus, data collection, and analysis methods were as described previously (*33*). Laser flash experiments were performed under pseudo-first-order conditions in anaerobiosis at room temperature. The flavins used were flavin mononucleotide (FMN), lumiflavin (LF), riboflavin (RF), and dRf. Standard solutions contained 0.1 mM flavin and 1 mM EDTA in 1.5 mL of 2 mM phosphate buffer, pH 7.0. When noted, aliquots of a concentrated NaCl solution were added to increase the ionic strength. C*c* reduction was monitored at 550 nm and the second-order rate constant ($k_2$) for protein reduction was calculated from the linear dependencies of the observed pseudo-first-order rate constant ($k_{obs}$) upon protein concentration. For most experiments, the error in $k_{obs}$ was estimated to be less than ±5%, based on reproducibility and signal-to-noise ratios. The ionic strength dependencies of the rate constants were analyzed by fitting the experimental data to the theoretical model for electrostatic interactions described by Watkins et al. (*34*), where a C*c* active-site radius of 5.5 Å was assumed. $k_2$ extrapolated to infinite ionic strength ($k_\infty$), as well as the charge of the protein active site ($Z$) and the electrostatic interaction energy ($V_{ii}$) between the reactants, were thus determined (*34*).

The kinetics of electron transfer from nonnitrated and nitrated C*c* species to horse C*c*O was also analyzed by laser flash spectroscopy following the flavin-mediated redox reactions, as previously described (*21, 35*). FMN was used to favor preferential C*c* reduction by the negatively charged flavin. The C*c*/C*c*O interaction was further monitored by following the absorbance changes at 550 and 604 nm, with respective contributions from C*c* and C*c*O predominantly arising (*21, 35, 36*). The standard reaction mixture contained, in a final volume of 0.8 mL, 10 mM Tris-HCl, pH 7.4, 10 mM KCl, 2 mM EDTA, 0.07% dodecyl $\beta$-maltoside, 0.1 mM FMN, 40 $\mu$M oxidized C*c*, and increasing amounts of C*c*O. All experiments were performed in anaerobiosis under pseudo-first-order conditions, with C*c*O well in excess over the reduced C*c* generated by the laser flash (<1 $\mu$M). Kinetic analyses were performed according to the reaction mechanisms previously proposed (*35, 37*).

*Activation of Caspases.* In vitro activation of caspases was achieved as described in ref *25*, with minor modifications. Briefly, an amount of cell extract equivalent to 100 $\mu$g of protein was preincubated for 60 min at 37 °C, in a total volume of 25 $\mu$L, with 25 mM KCl, 200 $\mu$M DTT, 200 $\mu$M dATP, and increasing concentrations of C*c*. After this first preincubation step, 180 $\mu$L of buffer A [10 mM HEPES, pH 7.0, with 50 mM NaCl, 40 mM $\beta$-glycerophosphate, 2 mM $MgCl_2$, 5 mM EGTA, 0.1 mg mL$^{-1}$ bovine serum albumin, and 0.1% (w/v) CHAPS], supplemented with 10 $\mu$M acetyl-Asp-Glu-Val-Asp-7-amino-4-methylcoumarin (Ac-DEVD-AMC), a fluorescent substrate specific for caspases 3/7, was added to the reaction mixture. Samples were then incubated for 45 min at 37 °C and the reaction was stopped by adding 100 $\mu$L of 175 mM acetic acid, 1% sodium acetate, and 500 $\mu$L of distilled water. The relative fluorescence of the samples was determined with 360 and 460 nm as excitation and emission wavelengths, respectively.

For experiments of coincubation, the samples were incubated under standard conditions, that is, with 5 $\mu$M nonnitrated C*c*, along with nitrated WT C*c* at increasing concentrations. For preincubation experiments, the samples were first preincubated for 10 min at 37 °C under standard conditions but with nonnitrated C*c* being substituted by nitrated C*c* at different concentrations; afterward, WT C*c* at 5 $\mu$M final concentration was added, and the samples were incubated as before.

## RESULTS AND DISCUSSION

The effects of tyrosine nitration have been studied in previous works with horse C*c* (*8, 12, 16, 23, 24*). However, only Radi's group (*23, 24*) has been able to separate the different nitrated C*c* variants from the nonnitrated form in order to fully characterize the modified protein, although the low amount of nitrated protein obtained prevented a complete study. Thus, important features such as redox potential of the nitrated form, time-resolved analysis of the reactivity of nitrated proteins, and effects of nitration of each individual tyrosine remain unsolved. Therefore, the effect of nitration on the properties of human C*c* has been here analyzed in purified preparations in order to elucidate how these changes affect its functionality, both in the respiratory electron transport chain and as a triggering agent in apoptosis. Nitrated horse C*c* has also been analyzed for comparative purposes.

*Construction of Mutants and Physicochemical Characterization of Different C*c *Variants, both Nonnitrated and Nitrated.* As shown in Figure 1, human C*c* contains five tyrosine residues, three of them (tyrosines 46, 48, and 67) close to the heme group and two others (tyrosines 74 and 97) far from the electron-transfer active site. To study the differential effect of nitration at each tyrosine residue, five mutants of the human heme protein have been constructed, in which all tyrosines but one have been replaced by phenylalanine. In addition, another mutant has been constructed with all tyrosines being replaced. The monotyrosine C*c* mutants are named h-Y46 (Y48F/Y67F/Y74F/Y97F),

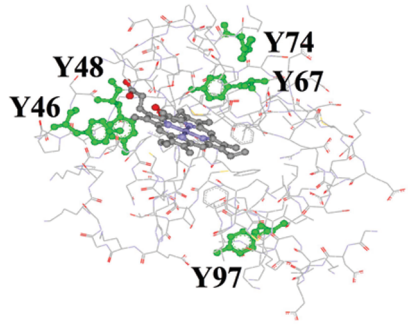


FIGURE 1: Three-dimensional structure of human C*c* (PDB code 1J3S) showing the location of the five tyrosine residues. Tyrosines are in green, and the heme group is in gray.

Table 1: Midpoint Redox Potential at pH 7.0 of Human and Horse WT C*c*, as Well as of the Monotyrosine Mutants of Human C*c*, in both Nonnitrated and Nitrated Forms

| | redox potential (mV) | |
|---|---|---|
| protein | native form | nitrated form |
| e-WT | 254.1 ± 5.7 | −130.6 ± 4.1 |
| h-WT | 262.4 ± 6.6 | −93.6 ± 5.8 |
| h-Y46 | 226.7 ± 5.6 | 164.3 ± 3.8 |
| h-Y48 | 220.5 ± 3.7 | 133.4 ± 26.3 |
| h-Y67 | 226.1 ± 5.5 | 252.8 ± 5.5 |
| h-Y74 | 209.3 ± 6.7 | 231.6 ± 17.6 |
| h-Y97 | 224.6 ± 8.0 | 230.3 ± 4.0 |
| h-Null | 216.5 ± 6.6 | 214.4 ± 16.3[a] |

[a] The null mutant cannot be nitrated because of the lack of any tyrosine residue, but the protein was subjected to the same treatment as the rest of mutants as a control. e-WT and h-WT are the horse and human WT proteins, respectively.

h-Y48 (Y46F/Y67F/Y74F/Y97F), h-Y67 (Y46F/Y48F/Y74F/Y97F), h-Y74 (Y46F/Y48F/Y67F/Y97F), and h-Y97 (Y46F/Y48F/Y67F/Y74F) to highlight the only tyrosine residue they bear. The mutant without tyrosines (null mutant, Y46F/Y48F/Y67F/Y74F/Y97F) was named h-Null.

None of the mutants shows drastic changes in its physicochemical characteristics, as expected from the conservative nature of the mutations. Thus, all the mutants show a slight decrease, of about 40 mV, in their midpoint redox potentials with respect to the WT C*c* (Table 1). In addition, the visible absorption spectrum of every mutant (except Y67, which shows WT features) exhibits a slight red shift of the α-band maximum of the reduced form, from 549.5 to 551 nm (data not shown). The secondary structure of the mutants seems to be also quite similar to WT C*c*, as deduced from the CD spectra (data not shown).

After bolus addition of peroxynitrite to C*c* samples, a mixture of nitrated and nonnitrated proteins is obtained (*8, 23, 24*). Here, we purified the nitrated fractions by taking advantage of the extra negative charge of the deprotonated tyrosyl anion—the p$K_a$ of which is significantly altered in the nitrated form by the strongly electron-withdrawing effect of the $NO_2$ substituent group when in the 3-position (*2, 8*)—thus allowing separation of the two forms of C*c* by CM-cellulose chromatography. Several nitrated fractions of WT C*c* were thus obtained (not shown), from which the most homogeneous one [with 3−4 nitrated tyrosines involving residues 46 or 48, 67, 74, and 97, as deduced by MALDI-TOF and peptide analysis (not shown)] was selected for this study. We found significant differences in the yield of nitration of different mutants (Table 2), and this could provide insights into the

Table 2: Yield of Nitration of the Human and Horse WT C*c* as Well as of the Five Monotyrosine Human Mutants[a]

| protein | h-Y46 | h-Y48 | h-Y67 | h-Y74 | h-Y97 | h-WT | e-WT |
|---|---|---|---|---|---|---|---|
| yield (%) | 4.5 | 4.9 | 15.5 | 16.4 | 8.3 | 17.8 | 23.5 |

[a] Values refer to the ratio between initial C*c* subjected to nitration and final nitrated C*c* recovered after the whole process of nitration and purification.

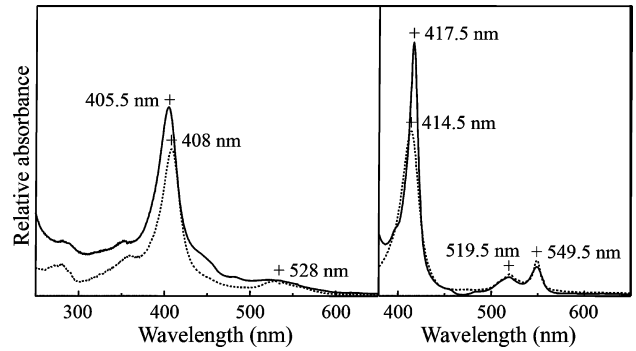


FIGURE 2: Absorption spectrum of oxidized (left) and reduced (right) human WT C*c*, either nonnitrated (—) or nitrated (---). The reaction cell contained 10 μM C*c* in 10 mM phosphate buffer, pH 7.0. After the spectrum of the oxidized form was recorded, the protein was reduced with dithionite, and thus the reduced nitrated form actually corresponds to aminated C*c*.

accessibility and nitration level of each tyrosine. Tyrosines 67 and 74 were the most easily nitrated, whereas tyrosines 46 and 48 were hardly modified, in agreement with previous studies with horse C*c* (*8, 16, 23*). In fact, the low nitration yield of mutants Y46 and Y48 prevented their functional characterization.

After nitration, all C*c* variants were in their oxidized states. The absorption spectrum of human WT C*c* was significantly altered (Figure 2). It is important to note that, in order to record the spectrum of the reduced form, dithionite, which also reduces the nitro group to the amino species (*29*), was added to the C*c* solution, and thus the spectrum shown corresponds to aminated C*c*. In the oxidized form, the shoulder with maximum at 455 nm corresponds to nitrotyrosine absorbance; this shoulder was hardly seen in previous spectra of nonpurified preparations (*8*). The Soret band of the spectrum presents the most relevant changes, with a displacement of the maximum from 408.5 to 405.5 nm in the oxidized state and from 414.5 to 417.5 nm in the reduced form (*8*). Moreover, the extinction coefficient in the maximum of this band is significantly higher in the nitrated form (Figure 2). The α and β bands of the reduced form show an extinction coefficient somewhat lower (28.9 $mM^{-1}$ $cm^{-1}$ for the α band) than the WT, although the maximum is preserved. The band at 680 nm of nitrated WT C*c* disappears (not shown), as previously described for nitrated horse C*c* (*8, 16, 23*). After nitration, minor changes of the CD spectra of most proteins were observed, indicating a slight increase in the α-helix content and a decrease in the nonregularly structured fraction.

As stated in the introduction, up to now there has not been a reliable value for the midpoint redox potential of nitrated C*c*, because of reduction of the nitro group to the amino species by the reductants used in the chemical titrations (*18*). By means of phototitrations with dRf as photosensitizer, thus avoiding the use of chemical reductants, the midpoint redox

potentials of the nitrated forms of all the C*c* variants have been accurately determined (Table 1). The redox potential value of human WT C*c* showed a drastic decrease of ca. 350 mV after nitration, with an even larger decrease for horse C*c* (Table 2). With respect to the mutants, none of the nitrated monotyrosine variants attains the lower redox potential value of the polynitrated WT protein: the redox potential values of h-Y46 and h-Y48 showed a significant decrease upon nitration, but they remained almost unchanged for the rest of the mutants.

From a physiological point of view, and when the drastic decrease in redox potential of the WT protein after nitration is taken into account, it is clear that polynitrated C*c* is unable to react with complex III, because the redox potential of cytochrome $c_1$, the exit port of electrons from the complex, is 230 mV, thus making the reaction thermodynamically unfeasible. This could lead to a positive feedback cycle for nitration, because in the event of a significant fraction of C*c* being nitrated, complex III would be partially blocked. Under such conditions, complex III will generate RNOS (*14, 38*), which in turn would yield nitrated C*c* so as to contribute to the blocking of complex III.

*Functional Characterization of Different* C*c Variants, both Nonnitrated and Nitrated.* With the changes induced in C*c* properties by nitration taken into account, the functionality of the different heme proteins has been analyzed by time-resolved absorption spectroscopy, to characterize the redox interaction of these proteins both with flavins and with their physiological acceptor C*c*O. Flavin-sensitized reduction of proteins by laser-flash kinetic spectroscopy has been shown to be a very powerful technique to study inter- and intramolecular electron transfer processes (*30*). By use of flavins bearing groups of different size and charge, the steric and electrostatic factors controlling the electron transfer process can be investigated (*30, 39*). In this work, a comparative study of the photoreduction of the different C*c*s by four different flavins has been performed. In all cases, the observed rate constants ($k_{obs}$) for reduction of C*c* by the different flavin semiquinones depended linearly on protein concentration, as shown in Figure 3 for FMN, allowing thus the determination of the bimolecular second-order rate constant ($k_2$) for the different interactions. From the ionic-strength dependence of $k_2$ for the reduction of C*c* by FMN, the observed rate constant extrapolated to infinite ionic strength ($k_\infty$), electrostatic interaction energy ($V_{ii}$), and charge of the active site ($Z$) can be estimated for each protein by applying the formalism developed by Watkins et al. (*34*). The resulting data are presented in Table 3. The nonnitrated mutants yielded values for the kinetic parameters similar to those for human WT C*c* (*21*), with the only exception of h-Y74, which shows a 2-fold increase in $k_2$ with most of the flavins. This finding indicates that the accessibility and electrostatic charge of the active site have not been significantly altered by the C*c* mutations.

Nitrated forms of C*c*s are less reactive toward flavins than native ones, presenting $k_2$ values 2−3 times lower. This effect is more evident with polynitrated horse C*c* (Table 3). These results indicate that nitration of tyrosines somewhat decreases the intrinsic reactivity of the proteins, most probably by means of steric hindrance. The exception is mutant h-Y97, whose nitrated form behaves in a way very similar to the nonnitrated form; this makes sense when the location of this tyrosine far from the electron transfer area of C*c* is taken into account (Figure 1). To rule out any secondary effect of nitration itself on protein reactivity, the h-Null mutant was subjected to the same process as the other species, and the so-treated protein showed the same reactivity as the nonnitrated one (Figure 3). It is also worth noting that the value of $Z$ of both human and horse WT C*c* becomes 1.5 units lower upon nitration, as expected from the extra negative charges close to the electron transfer area, arising from the partial negative charge of the nitro group and from the partial ionization of the tyrosyl groups at this pH. Among the mutants, only nitrated h-Y74 presents a similar decrease, suggesting that nitration of this particular tyrosine could be mainly responsible for the change in charge around the redox center (Table 3).

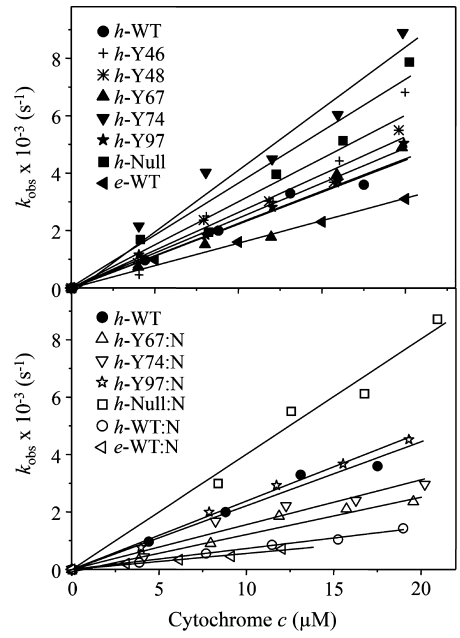


FIGURE 3: Dependence upon protein concentration of $k_{obs}$ for the reduction by FMN semiquinone of different C*c* variants in the nonnitrated (upper) and nitrated (**:**N) forms (lower). The reaction mixture contained, in a total volume of 1.5 mL, 2 mM phosphate buffer, pH 7.0, 1 mM EDTA, 100 $\mu$M FMN, and the indicated concentration of C*c*. The experiments were performed at room temperature. Other experimental conditions were as described under Experimental Procedures. The C*c* mutants containing just one tyrosine residue, with all the others replaced by phenylalanines, are named h-Y46, h-Y48, h-Y67, h-Y74, and h-Y97 to highlight the only remaining tyrosine residue. The h-Null mutant has all five tyrosines replaced by phenylalanine.

A flavin-mediated protocol to measure interprotein electron transfer was used to test the functionality of the mutants and the nitrated proteins, by following their oxidation by C*c*O purified from horse heart (*21, 34*). C*c*O reduction by horse C*c* was also measured for comparative purposes. All the mutants showed biphasic kinetics at 550 nm, with a major phase (up to 80% in amplitude) equivalent to the monophasic kinetics at 604 nm (not shown) and a minor slow phase; this was also the case for WT (Figure 4) (*21*). In agreement with previous works (*21, 34*), the kinetic analysis was focused on the fast predominant kinetic phase. Whereas both horse and WT human C*c* present a saturation profile for the dependence of $k_{obs}$ on C*c*O concentration (Figure 4), which is characteristic of a mechanism including transient complex formation before electron transfer (*21, 40*), all the nonnitrated

Table 3: Kinetic Parameters for Reduction by Flavin Semiquinones of Human and Horse WT C*c*, as Well as of the Monotyrosine and Null Mutants of Human C*c*, in both Their Nonnitrated and Nitrated (**:**N) States

| | LF | RF | dRf | FMN | | | |
|---|---|---|---|---|---|---|---|
| cytochrome | $k_2^a \times 10^{-8}$ ($M^{-1}$ $s^{-1}$) | $k_2^a \times 10^{-8}$ ($M^{-1}$ $s^{-1}$) | $k_2^a \times 10^{-8}$ ($M^{-1}$ $s^{-1}$) | $k_2^a \times 10^{-8}$ ($M^{-1}$ $s^{-1}$) | $k_\infty^{b,c} \times 10^{-7}$ ($M^{-1}$ $s^{-1}$) | $V_{ii}^c$ (kJ $mol^{-1}$) | $Z^c$ |
| h-WT | 0.98 | 0.90 | 14.50 | 2.23 | 1.49 | −10.0 | 5.1 |
| h-WT**:**N | 0.68 | 0.60 | 7.15 | 0.73 | 0.35 | −7.1 | 3.6 |
| h-Y46 | 1.29 | 1.02 | 7.37 | 3.01 | 0.81 | −8.9 | 4.6 |
| h-Y48 | 2.04 | 0.56 | 14.20 | 2.64 | 0.44 | −10.1 | 5.1 |
| h-Y67 | 1.56 | 1.33 | 11.90 | 2.41 | 0.46 | −9.9 | 5.1 |
| h-Y67**:**N | 0.40 | 0.32 | 2.66 | 1.28 | 0.20 | −10.6 | 5.5 |
| h-Y74 | 2.72 | 1.82 | 11.10 | 4.19 | 1.53 | −13.2 | 6.7 |
| h-Y74**:**N | 1.50 | 1.03 | 14.50 | 1.56 | 0.45 | −8.0 | 4.1 |
| h-Y97 | 1.83 | 1.38 | 10.70 | 2.43 | 1.48 | −10.2 | 5.2 |
| h-Y97**:**N | 1.86 | 0.91 | 12.40 | 2.38 | 0.34 | −14.8 | 7.6 |
| h-Null | 1.91 | 1.33 | 9.82 | 4.90 | 0.51 | −11.9 | 6.1 |
| h-Null**:**N[d] | 2.32 | 1.50 | 13.30 | 4.01 | 0.52 | −10.8 | 5.5 |
| e-WT | 0.79 | 0.59 | 6.55 | 1.57 | 0.54 | −9.9 | 5.1 |
| e-WT**:**N | 0.35 | 0.11 | 3.55 | 0.56 | 0.23 | −7.2 | 3.7 |

[a] Second-order rate constant for C*c* reduction at 60 mM ionic strength. [b] Second-order rate constant for C*c* reduction extrapolated to infinite ionic strength. [c] Values estimated according to the formalism developed in ref *34*. [d] These data correspond to the null mutant subjected to nitration treatment.

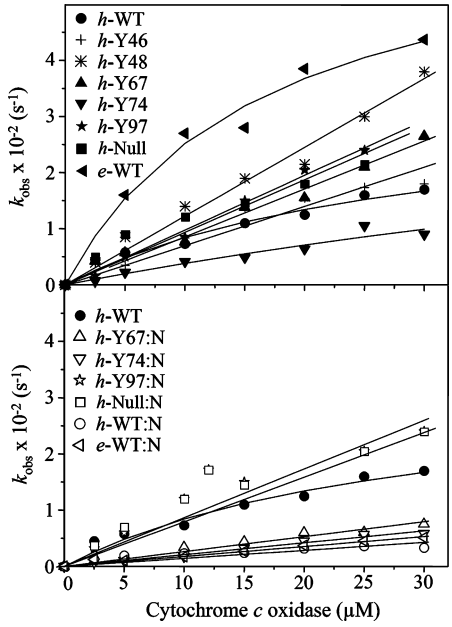


FIGURE 4: Dependence upon C*c*O concentration of $k_{obs}$ for oxidation of different C*c* species in the nonnitrated (upper) and nitrated (**:**N) (lower) forms. The reaction mixture contained (in a final volume of 0.8 mL) 10 mM Tris-HCl, pH 7.4, 2 mM EDTA, 0.07% dodecyl $\beta$-maltoside, 50 mM KCl, 100 $\mu$M FMN, and 40 $\mu$M C*c*. The experiments were performed at room temperature. The lines for h-WT and e-WT correspond to theoretical fittings by use of the formalism developed in ref *37*. Other experimental conditions were as described under Experimental Procedures.

mutants show a linear dependence of $k_{obs}$ on C*c*O concentration (Figure 4), indicating a second-order collisional process with no formation of any kinetically detectable electron-transfer complex. These data also indicate that the mutations (replacing four tyrosine groups in each case) are altering the bimolecular interaction step, which is a precisely tuned process very sensitive to changes, even subtle ones, in the interaction surface of the partners (*30, 41*). However, the $k_{obs}$ values were comparable in all cases. Because all the mutants behave in a similar way, this change of mechanism cannot be ascribed to the absence of any particular tyrosine but seems to be the result of an accumulative effect of mutations. The bimolecular rate constants can be directly calculated from the slope of the linear dependencies in Figure 4. Table 4 shows the values for $k_2$ with all the proteins. Although the different nature of the kinetic constants precludes a complete comparison of WT and the nonnitrated mutants, some mutants show higher $k_{obs}$ values than the WT C*c* at high C*c*O concentration, indicating that the complex formed by WT human C*c* with horse C*c*O is not optimized for electron transfer, as previously observed (*21*). In the nonnitrated form, all mutants present a reactivity equivalent to that of the h-Null mutant, with the noticeable exception of mutant h-Y74, which, in contrast to its high reactivity with flavins, shows the lowest kinetic parameters with C*c*O (Table 4), indicating that the presence of this tyrosine hinders the protein−protein interaction. Other significant differences exist between mutants h-Y48 and h-Y46. While these two mutants have a very similar pattern of mutations and show in every aspect very similar characteristics, they are, respectively, the fastest and slowest (after h-Y74) proteins in reacting with horse C*c*O.

Table 4: Kinetic Parameters for Oxidation by Horse C*c*O of Different C*c* Species[a]

| cytochrome | $k_2 \times 10^{-6}$ ($M^{-1}$ $s^{-1}$) | $K_A \times 10^{-4}$ ($M^{-1}$) | $k'_{et}$ ($s^{-1}$) |
|---|---|---|---|
| h-WT | | 3.7 | 301 |
| h-WT**:**N | 1.43 | | |
| h-Y46 | 7.00 | | |
| h-Y48 | 12.30 | | |
| h-Y67 | 8.56 | | |
| h-Y67**:**N | 2.65 | | |
| h-Y74 | 3.46 | | |
| h-Y74**:**N | 2.11 | | |
| h-Y97 | 9.77 | | |
| h-Y97**:**N | 8.65 | | |
| h-Null | 9.38 | | |
| h-Null**:**N | 7.95 | | |
| e-WT | | 6.0 | 680 |
| e-WT**:**N | 1.77 | | |

[a] $K_A$ and $k'_{et}$ values were estimated according to ref *37*.

When nitrated, the horse and WT human C*c*s present linear dependencies of $k_{obs}$ on C*c*O concentration (Figure 4), thus indicating that polynitration also modifies the interaction toward a collisional mechanism, as expected from modification of the interaction surfaces of both C*c*s. From the comparison of $k_{obs}$ for the interaction of nonnitrated and nitrated WT proteins with C*c*O, it is evident that reactivity is drastically diminished by nitration. This is just contrary

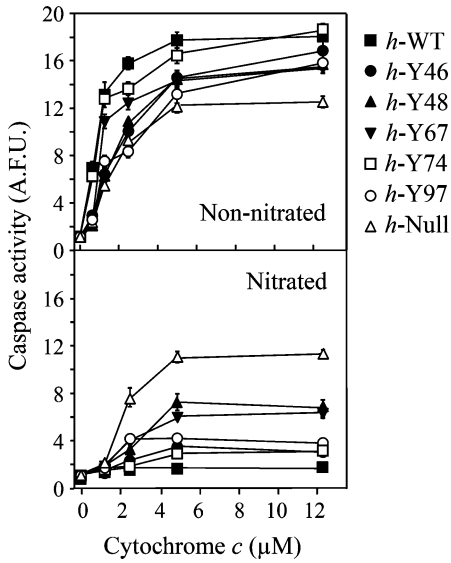


FIGURE 5: Activation of caspases in Jurkat cell extracts by human WT, h-Null mutant, or monotyrosine C*c*. (Upper panel) Each sample contained 100 $\mu$g of cell extracts and heme protein at varying concentration. (Lower panel) Same as above but the nitrated species of each heme protein was used. Other conditions were as described under Experimental Procedures.

to what is expected from the increase in driving force of the reaction due to the lower redox potential of nitrated proteins. Such a decrease in reactivity is a specific effect of nitration on the interaction with C*c*O, because the reactivity of the nitrated WT proteins with flavins was affected to a much lesser extent (Table 3). It is also worth noting that both nitrated WT forms present similar reactivity toward C*c*O, in contrast to the notably higher reactivity of horse C*c* in its nonnitrated form, indicating that horse C*c* is more affected by polynitration than human C*c*. In addition, the polynitrated forms of WT C*c*s show lower kinetic parameters than the mononitrated mutants (Table 4), thus indicating that the effect of nitration on reactivity with C*c*O seems to be accumulative, contrary to the effect observed in the reactivity with flavins, rather than the result of modifying any specific tyrosine group. With regard to the monotyrosine mutants, nitration of h-Y67 and h-Y74 promotes a significant decrease of the $k_2$ values for the interaction with C*c*O (up to 70% and 40%, respectively), while mutants h-Y97 and h-Null exhibit no significant change of reactivity (12% and 15% of decrease, respectively). Thus, the reactivity of mutants bearing nitrotyrosines 67 and, to a lesser extent, 74, is largely affected, indicating that the change of reactivity of the polynitrated WT protein is mainly due to nitration of these two tyrosine residues.

*Activation of Caspases by Different C*c *Variants, both Nonnitrated and Nitrated.* As stated in the introduction, nitrated C*c* has been proposed to act as an apoptosis signaler (*2, 15, 16*). However, some studies have shown that nitrated C*c* has a lower ability to activate caspases (*17, 18, 23*), suggesting that the modified protein is not fully functional in apoptosome assembly or operation. Thus, the ability of nitrated C*c* to activate caspases was first analyzed here.

As shown in Figure 5 (lower panel), Jurkat cell extracts preincubated with increasing concentrations of nitrated WT C*c* showed poor ability to activate caspases, as previously reported (*17, 18*). This diminished ability concerns both the concentration of nitrated C*c* required to saturate the caspase activity (5−10 times more) and the maximum activity level attained at saturating C*c* concentration (15% of the nonnitrated C*c*). Thus, nitrated C*c* has both a decreased affinity toward Apaf-1 (see also below) and a lower ability to form an active apoptosome. The differences between nonnitrated and nitrated C*c* were maintained when C*c* was preincubated at a fixed concentration with increasing levels of cell extracts (data not shown). The decrease in caspase activation is clearly not due to unspecific protein modifications arising from the treatment with peroxynitrite, as nonnitrated C*c* recovered after protein nitration behaved as the WT species (data not shown).

To assess whether the decreased efficiency of caspase activation of polynitrated WT C*c* is due to modification of any specific tyrosine residue, the reactivity of the monotyrosine mutants, both nonnitrated and nitrated, was also analyzed. The h-Null mutant, without any tyrosine residues, was also used as a control. Figure 5 (upper panel) shows that all the nonnitrated mutants conserved the ability to activate caspases: although slightly lower activation levels were observed, no drastic changes in the concentration of C*c* were required to saturate the process in all cases (Figure 5, upper panel), suggesting that tyrosines are not essential for caspase activation. The h-Y74 mutant showeded almost the same ability to activate caspases as WT, whereas the h-Null mutant showed the greatest alteration.

Nitration of the different monotyrosine C*c* mutants seriously affects their ability to activate caspases, but mainly by lowering the activity at saturating C*c* concentration while maintaining the saturation profile of the corresponding nonnitrated proteins (Figure 5, lower panel). This finding suggests changes in the ability to form an active apoptosome without influencing the C*c*−Apaf-1 interaction. Recent preliminary results obtained in a study with mononitrated horse C*c* show that the time course of activation of caspases by C*c* is significantly altered by nitration of tyrosine 74, whereas the effect of nitration of tyrosine 97 is much more modest (*23*). In our hands, the h-Null mutant, which was subjected to the same nitration process as a control, reached similar activation levels as the nontreated protein, demonstrating that the chemical treatment does not significantly affect the protein structure. Higher activities were obtained with the nitrated mutants h-Y48 and h-Y67 (ca. 50% compared to the nonmodified mutants), whereas the nitrated h-Y46, h-Y74, and h-Y97 proteins were more affected (ca. 25% compared to the nonmodified mutants). All these data suggest that the inhibitory effect on caspase activation observed with the polynitrated WT protein can be ascribed to the additive nitration of different tyrosine groups rather than to the specific nitration of any particular residue, as also observed with C*c*O.

In this context, nitration of the h-Y46, h-Y97, and in particular the h-Y74 mutant yields the greatest effects. As stated before, tyrosine residues at positions 46 and 74 are located at the surface of C*c*, near the heme group, whereas that at position 97 is on the opposite side of the protein. In particular, tyrosine 74 is close to lysine 72, which has an important role in the interaction of C*c* with Apaf-1 (*42, 43*). All these data indicate that the interaction with Apaf-1 takes place mainly through the heme side of C*c*, although there should be a global recognition of the whole molecule, as

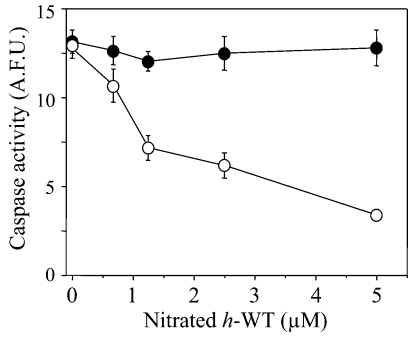


FIGURE 6: Competition between nonnitrated and nitrated C*c* to activate caspases. Jurkat cell extracts were either coincubated (●) with nitrated C*c* at varying concentrations and 5 $\mu$M nonnitrated C*c*, or preincubated (○) with varying concentrations of nitrated C*c* before the nonnitrated heme protein was added. Other conditions were as described under Experimental Procedures.

previously suggested (*43*−*45*). It is also noteworthy that the observed differences among the monotyrosine mutants were maintained when activation experiments were performed at different concentrations of KCl (data not shown).

From the results obtained with the different nitrated proteins, we conclude that the modified cytochromes cannot act as efficient apoptotic agents inducing apoptosome activation. On the contrary, nitrated C*c* could act as an apoptosis inhibitor by competing with the native protein by Apaf-1 binding. In agreement with the diminished affinity showed by the polynitrated WT C*c* (see above), coincubation of Jurkat cell extracts with both nitrated and nonnitrated WT C*c* did not interfere with caspase activation by the latter (Figure 6). However, when samples were briefly preincubated with polynitrated C*c* before the native protein was added, a significant decay in caspase activity was detected at increasing levels of nitrated C*c* (Figure 6). This finding suggests that polynitrated C*c* can interact with Apaf-1, although with less affinity, to induce certain conformational changes that could impair activation of caspases, as suggested previously for the (d)ATP exchange (*46*).

## CONCLUDING REMARKS

Nitration of WT C*c* drastically decreases both its reactivity with C*c*O and its ability to activate caspases, affecting both its affinity with Apaf-1 and the assembly of a functional apoptosome. This behavior can be ascribed to the additive effect of nitration of different tyrosine groups, rather than to the specific nitration of any particular residue. In summary, nitrated C*c* is not able to form an active apoptosome but impairs the respiratory electron-transfer process, contributing to increased RNOS production by mitochondria.

## ACKNOWLEDGMENT

We thank Pilar Alcántara for her technical assistance. dRf was a generous gift of Professor Gordon Tollin (University of Arizona, Tucson, AZ).

## REFERENCES

1. Kadenbach, B., Arnold, S., Lee, I., and Hüttemann, M. (2004) The possible role of cytochrome *c* oxidase in stress-induced apoptosis and degenerative diseases. *Biochim. Biophys. Acta 1655*, 400–408.
2. Radi, R. (2004) Nitric oxide, oxidants, and protein tyrosine nitration. *Proc. Natl. Acad. Sci. U.S.A. 101*, 4003–4008.
3. Orrenius, S. (2007) Reactive oxygen species in mitochondria-mediated cell death. *Drugs Metab. Rev. 39*, 443–455.
4. Cai, J., Yang, J., and Jones, D. P. (1998) Mitochondrial control of apoptosis: the role of cytochrome *c*. *Biochim. Biophys. Acta 1366*, 139–149.
5. Daniel, N. N., and Korsmeyer, S. J. (2004) Cell death: critical control points. *Cell 116*, 205–219.
6. Jiang, X., and Wang, X. (2004) Cytochrome *c*-mediated apoptosis. *Annu. Rev. Biochem. 73*, 87–106.
7. Pietraforte, D., Salzano, A. M., Marino, G., and Minetti, M. (2003) Peroxynitrite-dependent modifications of tyrosine residues in haemoglobin. Formation of tyrosyl radical(s) and 3-nitrotyrosine. *Amino Acids 25*, 341–350.
8. Cassina, A. M., Hodara, R., Souza, J. M., Thomson, L., Castro, L., Ischiropoulos, H., Freeman, B. A., and Radi, R. (2000) Cytochrome *c* nitration by peroxynitrite. *J. Biol. Chem. 275*, 21409–21415.
9. Jiao, K., Mandapati, S., Skipper, P. L., Tannenbaum, S. R., and Wishnok, J. S. (2001) Site-selective nitration of tyrosine in human serum albumin by peroxynitrite. *Anal. Biochem. 293*, 43–52.
10. Lin, H. L., Myshkin, E., Waskell, L., and Hollenberg, P. F. (2007) Peroxynitrite inactivation of human cytochrome P-450s 2B6 and 2E1: heme modification and site-specific nitrotyrosine formation. *Chem. Res. Toxicol. 20*, 1612–1622.
11. Castro, L., Eiserich, J. P., Sweeney, S., Radi, R., and Freeman, B. A. (2004) Cytochrome *c*: a catalyst and target of nitrite-hydrogen peroxide-dependent protein nitration. *Arch. Biochem. Biophys. 421*, 99–107.
12. Ueta, E., Kamatani, T., Yamamoto, T., and Osaki, T. (2003) Tyrosine-nitration of caspase 3 and cytochrome *c* does not suppress apoptosis induction in squamous cell carcinoma cells. *Int. J. Cancer 103*, 717–722.
13. Schonhoff, C. M., Gaston, B., and Mannick, J. B. (2003) Nitrosylation of cytochrome *c* during apoptosis. *J. Biol. Chem. 278*, 18265–18270.
14. Szabó, C., Ischiropoulos, H., and Radi, R. (2007) Peroxynitrite: biochemistry, pathophysiology and development of therapeutics. *Nature 6*, 662–680.
15. Kagan, V. E., Tyurin, V. A., Jiang, J., Tyurina, Y. Y., Ritow, V. B., Amoscato, A. A., Osipov, A. N., Belikova, N. A., Kapralov, A. A., Kini, V., Vlasova, I. I., Zhao, Q., Zou, M., Di, P., Svistunenko, D. A., Kurnikov, I. V., and Borisenko, G. G. (2005) Cytochrome *c* acts as a cardiolipin oxygenase required for release of proapoptotic factors. *Nat. Chem. Biol. 1*, 223–232.
16. Jang, B., and Han, S. (2006) Biochemical properties of cytochrome *c* nitrated by peroxynitrite. *Biochimie 88*, 53–58.
17. Oursler, M. J., Bradley, E. W., Elfering, S. L., and Giulivi, C. (2005) Native, not nitrated, cytochrome *c* and mitochondria-derived peroxide drive osteoclast apoptosis. *Am. J. Physiol. Cell Physiol. 288*, C156–C168.
18. Nakagawa, H., Komai, N., Takusagawa, M., Miura, Y., Toda, T., Miyata, N., Ozawa, T., and Ikota, N. (2007) Nitration of specific tyrosine residues of cytochrome *c* is associated with caspase-cascade inactivation. *Biol. Pharm. Bull. 30*, 15–20.
19. Koeck, T., Fu, X., Hazen, S. L., Crabb, J. W., Stuehr, D. J., and Aulak, K. S. (2004) Rapid and selective oxygen-regulated protein tyrosine denitration and nitration in mitochondria. *J. Biol. Chem. 279*, 27257–27262.
20. Kamisaki, Y., Wada, K., Bian, K., Balabanli, B., Davis, K., Martin, E., Behbod, F., Lee, Y., and Murad, F. (1998) An activity in rat tissues that modifies nitrotyrosine-containing proteins. *Proc. Natl. Acad. Sci. U.S.A. 95*, 11584–11589.
21. Rodríguez-Roldán, V., García-Heredia, J. M., Navarro, J. A., Hervás, M., De la Cerda, B., Molina-Heredia, F. P., and De la Rosa, M. A. (2006) A comparative kinetic analysis of the reactivity of plant, horse, and human respiratory cytochrome *c* towards cytochrome *c* oxidase. *Biochem. Biophys. Res. Commun. 346*, 1108–1113.
22. Schmidt, T. R., Wildman, D. E., Uddin, M., Opazo, J. C., Goodman, M., and Grossman, L. I. (2005) Rapid electrostatic evolution at the binding site for cytochrome *c* on cytochrome *c* oxidase in anthropoid primates. *Proc. Natl. Acad. Sci. U.S.A. 102*, 6379–6384.
23. Souza, J. M., Castro, C., Cassina, A. M., Batthyány, C., and Radi, R. (2008) Nitrocytochrome *c*: synthesis, purification, and functional studies. *Methods Enzymol. 441*, 197–215.
24. Batthyány, C., Souza, J. M., Durán, R., Cassina, A., Cerveñansky, C., and Radi, R. (2005) Time course and site(s) of cytochrome *c* tyrosine nitration by peroxynitrite. *Biochemistry 44*, 8038–8046.

25. Keller, P., Schaumburg, F., Fischer, S. F., Häcker, G., Gross, U., and Lüder, C. G. (2006) Direct inhibition of cytochrome *c*-induced caspase activation in vitro by *Toxoplasma gondii* reveals novel mechanisms of interference with host cell apoptosis. *FEMS Microbiol. Lett. 258*, 312–319.
26. Beckman, J. S., Ischiropoulos, H., Zhu, L., van der Woerd, M., Smith, C., Chen, J., Harrison, J., Martin, J. C., and Tsai, M. (1992) Kinetics of superoxide dismutase and iron-catalyzed nitration of phenolics by peroxynitrite. *Arch. Biochem. Biophys. 298*, 438–445.
27. Soulimane, T., and Buse, G. (1995) Integral cytochrome-*c* oxidase. Preparation and progress towards a three-dimensional crystallization. *Eur. J. Biochem. 227*, 588–595.
28. Yoshikawa, S., Choc, M. G., O'Toole, M. C., and Caughey, W. S. (1977) An infrared study of CO binding to heart cytohrome *c* oxidase and hemoglobin A. *J. Biol. Chem. 252*, 5498–5508.
29. Sokolovsky, M., Riordan, J. F., and Vallee, B. L. (1967) Conversion of 3-nitrotyrosine to 3-aminotyrosine in peptides and proteins. *Biochem. Biophys. Res. Commun. 27*, 20–25.
30. Tollin, G. (1995) Use of flavin photochemistry to probe intraprotein and interprotein electron transfer mechanisms. *J. Bioenerg. Biomembr. 27*, 303–309.
31. Appleby, C. A. (1969) Electron transport systems of *Rhizobium japonicum*. II. *Rhizobium* haemoglobin, cytochromes and oxidases in free-living (cultured) cells. *Biochim. Biophys. Acta 172*, 88–105.
32. Sreerama, N., and Woody, R. W. (2000) Estimation of protein secondary structure from CD spectra: comparison of CONTIN, SELCON and CDSSTR methods with an expanded reference set. *Anal. Biochem. 282*, 252–260.
33. Navarro, J. A., Hervás, M., Pueyo, J. J., Medina, M., Gómez-Moreno, C., De la Rosa, M. A., and Tollin, G. (1994) Laser flash-induced photoreduction of photosynthetic ferredoxins and flavodoxin by 5-deazariboflavin and by a viologen analogue. *Photochem. Photobiol. 60*, 231–236.
34. Watkins, J. A., Cusanovich, M. A., Meyer, T. E., and Tollin, G. (1994) A "parallel plate" electrostatic model for bimolecular rate constants applied to electron transfer proteins. *Protein Sci. 3*, 2104–2114.
35. Hazzard, J. T., Rong, S. Y., and Tollin, G. (1991) Ionic strength dependence of the kinetics of electron transfer from bovine mitochondrial cytochrome *c* to bovine cytochrome *c* oxidase. *Biochemistry 30*, 213–222.
36. Navarro, J. A., Durán, R. V., De la Rosa, M. A., and Hervás, M. (2005) Respiratory cytochrome *c* oxidase can be efficiently reduced by the photosynthetic redox proteins cytochrome $c_6$ and plastocyanin in cyanobacteria. *FEBS Lett. 579*, 3565–3568.
37. Meyer, T. E., Zhao, Z. G., Cusanovich, M. A., and Tollin, G. (1993) Transient kinetics of electron transfer from a variety of *c*-type cytochromes to plastocyanin. *Biochemistry 32*, 4552–4559.
38. Chen, Q., Vazquez, E. J., Moghaddas, S., Hoppel, C. L., and Lesnefsky, E. J. (2003) Production of reactive oxygen species by mitochondria: central role of complex III. *J. Biol. Chem. 278*, 36027–36031.
39. Meyer, T. E., Watkins, J. A., Przysiecki, C. T., Tollin, G., and Cusanovich, M. A. (1984) Electron-transfer reactions of photoreduced flavin analogues with *c*-type cytochromes: quantitation of steric and electrostatic factors. *Biochemistry 23*, 4761–4767.
40. Hervás, M., Navarro, J. A., Díaz, A., Bottin, H., and De la Rosa, M. A. (1995) Laser-flash kinetic analysis of the fast electron transfer from plastocyanin and cytochrome $c_6$ to photosystem I. Experimental evidence on the evolution of the reaction mechanism. *Biochemistry 34*, 11321–11326.
41. Hope, A. B. (2000) Electron transfer amongst cytochrome *f*, plastocyanin and photosystem I: kinetics and mechanisms. *Biochim. Biophys. Acta 1456*, 5–26.
42. Kluck, R. M., Ellerby, L. M., Ellerby, H. M., Naiem, S., Yaffe, M. P., Margoliash, E., Bredesen, D., Mauk, A. G., Sherman, F., and Newmeyer, D. D. (2000) Determinants of cytochrome *c* pro-apoptotic activity. The role of lysine 72 trimethylation. *J. Biol. Chem. 275*, 16127–16133.
43. Yu, T., Wang, X., Purring-Koch, C., Wei, Y., and McLendon, G. L. (2001) A Mutational epitope for cytochrome *c* binding to the apoptosis protease activation factor-1. *J. Biol. Chem. 276*, 13034–13038.
44. Acehan, D., Jiang, X., Morgan, D. G., Heuser, J. E., Wang, X., and Akey, C. W. (2002) Three-dimensional structure of the apoptosome: implications for assembly, procaspase-9 binding, and activation. *Mol. Cell 9*, 423–432.
45. Bao, Q., and Shi, Y. (2007) Apoptosome: a platform for the activation of initiator caspases. *Cell Death Differ. 14*, 56–65.
46. Kim, H. E., Du, F., Fang, M., and Wang, X. (2005) Formation of apoptosome is initiated by cytochrome *c*-induced dATP hydrolysis and subsequent nucleotide exchange on Apaf-1. *Proc. Natl. Acad. Sci. U.S.A. 102*, 17545–17550.

BI801329S